Dendritic growth in two-dimensional smectic E freely suspended film

Journal:	*Molecular Systems Design & Engineering*
Manuscript ID	ME-ART-01-2020-000006.R1
Article Type:	Paper
Date Submitted by the Author:	20-Feb-2020
Complete List of Authors:	Yoon, Dong Ki; KAIST, Department of Chemistry; KAIST, Graduate School of Nanoscience and Technology Zhu, Chenhui; Lawrence Berkeley National Laboratory, Advanced Light Source Kim, Yun Ho; Korea Research Institute of Chemical Technology, Division of Advanced Materials Shen, Yongqiang; University of Colorado, Department of Physics and FLCMRC Jung, Hee-Tae; Korea Advanced Institute of Science and Technology, Department of Chemical + Biomolecular Engineering Clark, Noel; University of Colorado, Department of Physics and FLCMRC

Liquid crystal (LC) materials have been interested in material science and technologies due to the promising applications in display and sensing applications. Recently, it was reported that the high charge carrier mobility can be obtained using small molecular weight LC organic semiconducting materials that have the smectic E phase. However, there has barely studied about the basic smectic E phase structures though the X-ray and electron diffraction structural studies had been carried out to show a two-dimensional hexagonal lattice and strong herringbone packing. Here, we have investigated the dendritic growth of freely suspended film of the smetic E, which can make easy to see the specific arrangement of LC molecules. This can be understood based on packing sequence of orthorhombic unit cell and molecular packing of the LC molecules in the smectic E phase. Quantitative measurement of the dendritic branch meets the value theoretically predicted using universal growth laws. Our resultant work can suggest a hint to improve the electrical property of the organic electronics in the future.

ARTICLE

Dendritic growth in two-dimensional smectic E freely suspended film

Received 00th January 20xx,
Accepted 00th January 20xx

DOI: 10.1039/x0xx00000x

Dong Ki Yoon[*ab], Chenhui Zhu[c], Yun Ho Kim[de], Yongquang Shen[f], Hee–Tae Jung[g], and Noel A. Clark[*f]

We have investigated the dendritic growth of freely suspended film of a rod-type molecule forming the smectic E phase from the smectic A phase upon cooling from isotropic temperature. In contrast to the fractal growing patterns of other smectic liquid phases, this exhibits a clear dendritic growth along with the director of the molecular unit cell of the smectic E phase. As freezing from the outmost monolayers of the freely suspended film, the sequential dendritic growth occurs based on the confining effect of preformed outer layers of the smectic E phase. Analysis for the growth law of the characteristic length; $L(t) \sim t^n$ shows that the growth process is consistent with the theoretically predicted (n~0.66).

.

Introduction

The freely suspended film of soft condensed matters in promoting order or disorder has been widely studied because of the reduced structural dimensionality.[1-6] Two-dimensional melting and freezing, surface-induced, and layer-by-layer transitions are examples of the wide range of phenomena that have been investigated in such freely suspended films. Among these, surface melting and freezing of the liquid crystals (LCs) on the substrates such as glass and metal has been massively studied because of the practical demand,[7,8] while the freely suspended film of LC materials has not been much studied although in many cases more ordered behaviour is shown than the bulk, in which surface freezing can be observed.[9-11] Especially, the relevant smectic LCs are excellent model systems to study these two-dimensional growing phenomena and phase transitions and critical fluctuations in the LC phases.

It is also well known that the smectic LC structures are built up by orientational ordering if there are the translational disordered smectic layers within these, which form more ordered phases such as hexatic phases, the polarization splay modulated (B7) phases and the helical nanofilament (B4) phase.[12-15] This structural ordering can be increased as temperature decreases in the smectic layers, meaning that a layer structure without order (smectic A (SmA), SmC) within the layers can pass over with decreasing temperature by phase transitions to layer structures with orders in the layers (SmB, SmE, etc).[16-18] Whereas the smectic phases of SmA and SmC types have been studied before,[19-21] the structure observation of the highly ordered smectic phase such as the SmE phase which is a layered phase with the molecules oriented perpendicular to the layer plains and hexagonally ordered within each layer, are restricted to a few classes of substances. The X-ray and electron diffraction studies demonstrated this hexagonal order in materials,[22-24] confirming that the SmE phase is characterized by a two-dimensional hexagonal lattice and strong herringbone packing.

Here we report the dynamic growth in the freely suspended film of the SmE phase, which is now the essential phase to show the high charge carrier mobility.[25-27] Even though the dynamics in the growth of thick film between planar aligned substrates was studied before, both theoretically and experimentally,[28-31] there has not been studied about the dendritic growth in freely suspended film of the SmE phase. To understand the dynamic growth of the SmE phase, we probe the freely suspended film by DTLM (depolarized transmission light microscopy) at a certain temperature range between the smectic Ã phase (i.e., a SmÃ phase that has body-centred rectangular domains;[32] from here SmÃ will be alternated to SmA for the convenience) and the SmE phase. The feely suspended film explored here has several layers, approximately ~ 6 layers because the birefringence is not so strong to be considered at most ~ 10 layers. It is expected that this basic structural analysis of the SmE film will extend the realm of smectic LCs to organic electronics for the next generation opto-electronic devices.

[a]Department of Chemistry, KAIST, Daejeon 34141 Korea
[b]Graduate School of Nanoscience and Technology and KINC, KAIST, Daejeon 34141, Korea,
[c]Advanced Light Source, Lawrence Berkeley National Laboratory, Berkeley, CA 94720, USA,
[d]Advanced Materials Division, Korea Research Institute of Chemical Technology, Daejeon 34114, Korea,
[e]Chemical Convergence Materials and Processes, KRICT School, University of Science and Technology, Daejeon, 34113, Korea,
[f]Department of Physics and Soft Materials Research Center University of Colorado Boulder, CO 80309, USA,
[g]Department of Chemical and Biomolecular Engineering, KAIST, Daejeon 34141, Korea

Results and discussion

To achieve our goal, firstly, a rod-shaped liquid crystalline material, **Y002**, was synthesized according to the method previously reported.[33] The thermal phase transition of **Y002** happens upon cooling from the isotropic to the SmA phase at T = 185°C, and then from the SmA to the SmE phase at T = 111°C (Fig. 1a).[34-36] The semi-fluorinated tails of **Y002** cause splayed molecular stacking, as shown in Fig. 1b, which depends on dipole delocalization, showing the orthorhombic configuration of **Y002** molecules with a herringbone arrangement. The unit cell shows the short molecular dimension of a=6.8 nm, b=5.6 nm, and c=7.3 nm (Fig. 1b). This typical SmE phase is resulted from the attractive pi stacking interaction between adjacent biphenyl groups and shows sufficient dense-packed molecules per unit cell.

Two-dimensional dendritic growths of the freely suspended film of the SmE phase from the SmA phase were directly investigated by in-situ imaging of DTLM. Here, 5° depolarization between cross-polarisers was used because of the low birefringence of optical morphologies during transition between the SmA and the SmE. The film is made in the SmA phase, in which it is hard to see the specific optical anisotropy because the SmA phase is uniaxial on top view in the given experimental condition (Fig. 2a). As the SmA film transits to the SmE film upon cooling, a dim birefringent structure having saw-tooth like morphology is growing from right side to the left side, which results from the dendritic growth of biaxial units of the SmE film (Fig. 2b-d). Once this growing is saturated, we hardly see the saw-tooth-like structure because the domains near each boundary are merged; instead, there appear sharp lines between domains that depend on the orientation of the biaxial SmE phase of **Y002** molecules (Fig. 2e). Finally, the dendritic growth of the SmE phase occurs legitimately from right to left as a function of time. Now, various birefringent optical morphologies of different domains can be observed (Fig. 2e, f).

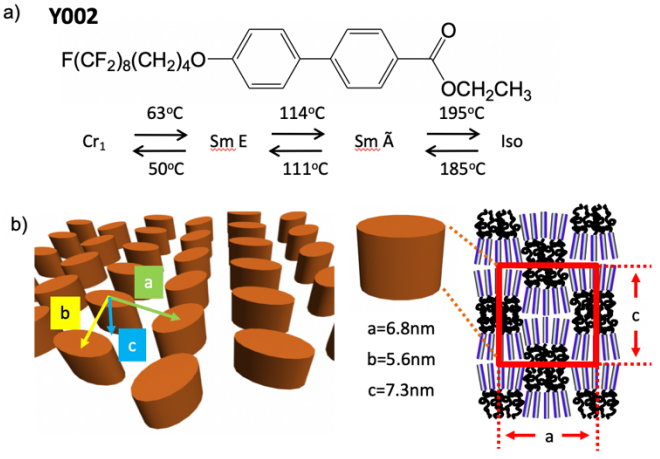

Fig. 1 Phase transition of **Y002** and molecular ordering. (a) The chemical structure and phases of liquid crystal, **Y002** with transition temperatures. (b) Orthorhombic packing structure of the SmE phase of **Y002** with herringbone arrangement in which the unit cell shows the short molecular dimension of a=6.8 nm, b=5.6 nm and c=7.3 nm.

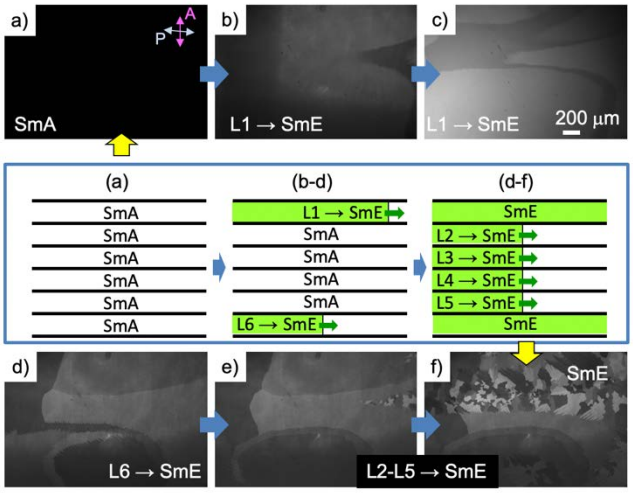

Fig. 2 Two-dimensional dendritic growths of the freely suspended film of the SmE phase from the SmA phase on cooling and their schematic representations. Here, 5° depolarization between cross-polarizers is used because of the low transmitted intensity. (a) There's little birefringent signal because the SmA phase is uniaxial on top view. (b-d) As the phase transition goes from the SmA phase to the SmE phase, the morphological changes happen from the two outmost layers of freely suspended film (L1 and L6). (e, f) Once the phase transition in the outer layers is finished, the internal SmA phase freezes into the SmE phase with dendritic growing tendency. Especially, the dendritic branches have 90° each other in one domain, regardless of dark and bright region. Schematic representation of the possible scenario for the transition of a multi-layer SmA film into the SmE film through layer-by-layer surface transition.

Interestingly, each branch in one domain is growing regularly with 90° difference between main and side branches, regardless of dark or white one, meaning that different orientation of the SmE domains.

The dynamic structural behaviour of layer-by-layer freezing during SmA to SmE transition shows that there are three possible processes in which a SmA film can freeze into a SmE film upon cooling, as represented schematically in Fig. 2 for the six-layer film. The two outermost layers of L1 and L6 firstly freeze into the SmE phase, while the interior four layers remain in the SmA phase (Fig. 2b-d). Then the next interior layers of L2-L5 transform into the SmE phase sequentially, and finally, all six layers are in the SmE phase (Fig. 2e, f). Since the SmE phase shows pseudo-three-dimensional structures, we can guess that the role it plays, if any, in the surface freezing of the SmA phase depends primarily on the extent to which the smectic layers are coupled to each other. Additional discussion on the correlation between the interlayer coupling and the type of surface transitions will be described to clarify this later in this paper.

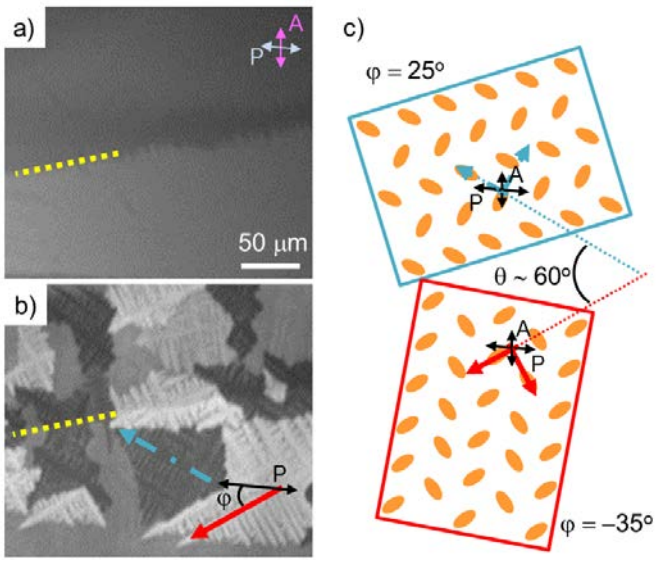

Fig. 3 The enlarged images of each specific transition point of freely suspended film during phase transition from the SmA to the SmE phase, and representative schematic sketch. (a) Upon cooling, saw-tooth like morphologies are appeared as the SmA phase transforms into the SmE phase, yellow dashed line means the boundary of different domains in the two outmost layers of the SmE phase. (b) The dendritic branches have 90° each other in a domain, while it shows 60° between each domain (red solid and blue dotted line). (c) 90° dendritic growth is based on the herringbone packed unit cell (orange ellipsoids) of the SmE phase. The difference in angle of 60° between each domain can explain the difference in optical birefringence.

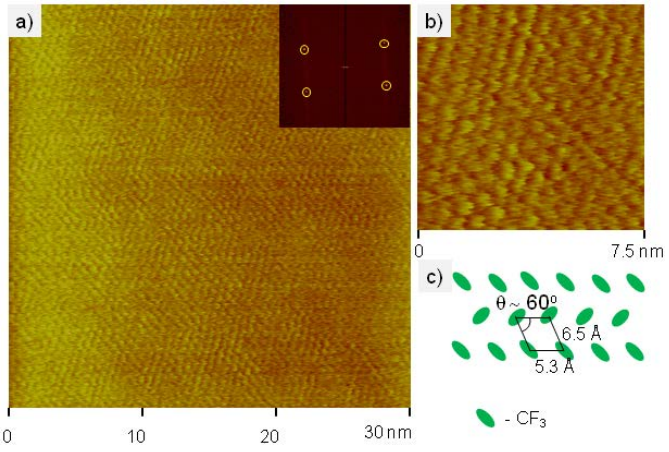

Fig. 4 Molecular resolution AFM images of Langmuir monolayer film. (a, b) Top-view of the Langmuir monolayer shows hexagonal packed $–CF_3$s. (c) Each unit has 60° between neighboring units, meaning distance between the semi-fluoroalkyl chains of ~ 0.50 nm.

Because of the strong intrinsic herringbone ordering in the SmE phase, a model of freely suspended film of **Y002** could be formulated for a LC structure with coupled herringbone and bond-orientational degrees of freedom (Fig. 3). With this model, it is possible to understand the peculiar behaviour at the SmA-SmE phase transition. This model can be obtained based on the enlarged images of each specific transition point of freely suspended film during transition of SmA to SmE phase. As the SmA phase transforms to the SmE phase, firstly, the two outermost layers (L1 and L6 in Fig. 2) freeze and then all of interior layers (L2-L5) change into the SmE phase sequentially, and such certain birefringent changes can be seen clearly in Fig. 3a and b. During this process, there are growing a few kinds of domains of dark and bright morphologies although it is not easy to be distinguished in Fig. 3a. But 90° growing dendritic branches of each domain can be clearly seen in Fig. 3b, and simply we can recognize the similar growing morphologies of dark and bright domains. From this, there are three things to be considered. Firstly, 90° growth of each branch is caused by the orthorhombic unit cell in connection with a herringbone packing as shown in Fig. 1b and 3c. Each unit cell has 90° difference and this generates the macroscopic dendritic growth of the SmE domains. Secondly, the different contrast of dark and bright region is resulted from the transmitted light intensity that depends on the $sin^2 2\varphi$, where φ is the angle between a principal optic axis and the polarization direction (Fig. 3b and c). This can explain the reason why the domain of φ~35° shows brighter than that of $\varphi \sim 25°$ by Malus's law, in which a linearly polarized light whose polarizing direction is relatively parallel to the axis of the polarizer can show a high transmitted intensity (Fig. 3c).[37] Thirdly, considering the angle (θ) between bright and dark domains is about 60°, and this can be explained based on the packing sequence of **Y002** molecules. Molecular resolution AFM image of a monolayer film of **Y002** (Fig. 4) made by Langmuir method shows top-view of the herringbone type packed chemical functionalities of "$–CF_3$", revealing 60° between neighbouring "$-CF_3$" units (Fig. 4c).[38] This packing sequence governs the propagation of dendritic growth after the nucleation of each domain.

The freezing process during the phase transition is of fundamental importance for the processing of materials, ranging from metal alloys and glasses to polymers. Thermal fluctuations of the unstable interface between the SmA phase and the SmE phase result from the competition between a temperature gradient or chemical potential gradient, inducing the nucleation of the low-temperature phase,[39,40] here the SmE, and domains of dendritic branches in the SmE phase grow spontaneously once a critical nucleus size is exceeded. When nucleus growth is followed optically, the time evolution of the characteristic length, L(t) of one of dendritic branches as a function of time can be described by a universal growth law, $L(t) \sim t^n$, where n is called the growth exponent.[41,42] During the growth, each domain of the SmA and the SmE phase is separated by a sharp domain boundary and the velocity of the local domain interface is equal to the local curvature of the domain. The general result (n ~ 0.5) of this problem at a certain quench depth (i.e. the difference of temperature between phases; ΔT=0 K) was already obtained.[43,44] And this n value can be varied by ΔT; for 0K < ΔT < 0.8K, n value is 0.5 < n < 1.0.[45-47] From analysis of various images as a function of time, the dendritic growth in free-standing film of SmE phase can be quantified by L(t) based on the growing area, in which the area is translated to the length of one branch (Fig. 5). The latter time regime of the dendritic domain growth in Fig. 2 (d~f) can clearly

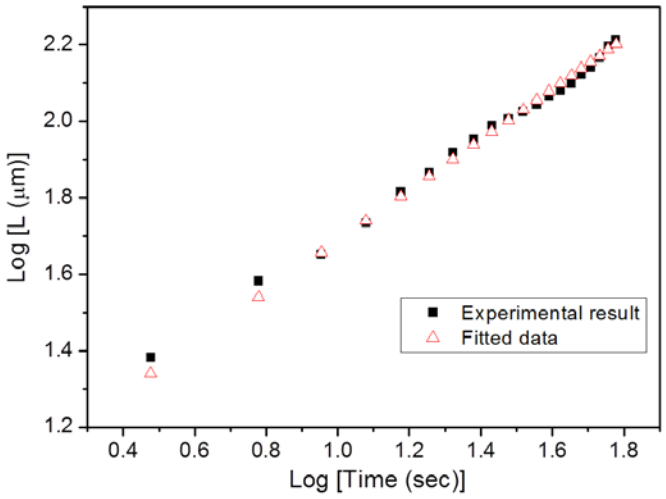

Fig. 5 Characteristic length L(t) of a dendritic branch (black squares) based on the experimental results and fitted data (red triangles). Growth exponent n is determined from this fitting and the value is ~ 0.66.

be identified by a change of slope in the representation of L(t) versus t used for the determination of the growth exponents (n). Therefore, considering our quench depth (ΔT) is ~ 0.3, n is determined 0.66 after fitting (red triangles) based on the experimental data (black squares) as described in Figure 5. As dendritic growth is saturated to meet the other domains, L(t) becomes constant on these contacts.

Conclusions

In summary, we have investigated the dynamics of the dendritic growth of free-standing film, during freezing from the SmA phase to the SmE phase. This specific dendritic growing process can be understood based on packing sequence of orthorhombic unit cell and molecular packing of the SmE phase of **Y002**. Quantitative measurement of the dendritic branch meets the value theoretically predicted based on universal growth laws of the $L(t) \sim t^n$, here n is ~ 0.66. Considering the SmE phase is the one of the promising phases that can show the high charge carrier mobility, our resultant work can suggest a hint to improve the electrical property of the organic electronics in the future .

Conflicts of interest

There are no conflicts to declare.

Experimental details

Materials

The LC material **Y002** was synthesized by the procedure for the alkylation of methyl ethyl 4′-hydroxy-4-biphenyl carboxylate with 1H,1H,2H,2H,3H,3H,4H,4Hperfluorododecyl bromide in DMF (Sigma Aldrich, 99.8%) at 70 ˚C under reflux with K_2CO_3.[32]

Sample Preparation and optical characterization

The freely suspended film was made by using a circular hole in a glass coverslip that has 18 x 18 mm^2 and thickness of ~ 0.15 mm. A small amount of **Y002**, ~ a few tens of mg was placed near the hole of a coverslip and then heated up to the SmA phase then spread with the other glass sip to make the freely suspended film in the hole.[1] For this, a heating stage and temperature controller (Instec STC200) was used, and DTLM (Olympus BX51) was used to observe the dendritic growth of **Y002** on cooling to the SmE phase.

Langmuir monolayer investigation

Langmuir monolayer was prepared using a commercial Langmuir trough (NIMA, Coventry, England). A dilute solution of **Y002** in ethyl acetate (5μl, 1mg of molecule/ml, Merck, HPLC grade) was spread on an ultra-pure water (Milli-Q; resistivity ca. 18.2MΩcm) subphase and the monolayer was deposited on mica substrate. Surface topography of the monolayer of **Y002** was performed under ambient conditions with an AFM (Nanoscope Ⅲ: Veeco Instruments, Santa Barbara, CA). For the molecular resolution mode and preventing from deformation of sample, contact mode AFM with Si_3N_4 cantilevers having a nominal spring constant of 0.06 N/m was used.

Acknowledgments

This was supported by the KAIST Grand Challenge 30 Project (KC30) and the National Research Foundation (NRF) funded by the Korean Government (MIST) (2017R1E1A1A01072798). Experiments at the PLS-II were supported in part by MIST and Pohang University of Science and Technology. It was also supported by the Soft Materials Research Center under US NSF MRSEC Grant DMR-1420736.

References

1 Z. H. Nguyen, C. S. Park, J. Pang, and N. A. Clark, *Proc. Natl. Acad. Sci. U.S.A*, 2012, **109**, 12873.
2 C. Y. Young, R. Pindak, N. A. Clark, and R. B. Meyer, *Phys. Rev. Lett*., 1978, **40**, 773.
3 R. Pindak, C. Y. Young, R. B. Meyer, and N. A. Clark, *Phys. Rev. Lett.,* 1980, **45**, 1193.
4 J. Doucet, A. M. Levelut, M. Lambert, L. Liebert, and L. Strzelecki, *J. Phys. (Paris),* 1975, **36**, C1-13.
5 C. F. Chou, A. J. Jin, S. W. Hui, C. C. Huang, and J. T. Ho, *Science,* 1998, **280**, 1424.
6 A. A. Sonin, Freely Suspended Liquid Crystalline Films, Wiley, 1999.
7 R. Geer, T. Stoebe, C. C. Huang, R. Pindak, G. Srajer, J.W. Goodby, M. Cheng, J. T. Ho, and S. W. Hui, *Phys. Rev. Lett.,* 1991, **66**, 1322.
8 P.J. Collings, *Liquid Crystals,* Princeton University Press, 2002.
9 C. Y. Chao, C. F. Chou, J. T. Ho, S. W. Hui, A. J. Jin, and C. C. Huang, *Phys. Rev. Lett*., 1996, **77**, 2750.
10 R. Pindak, D. J. Bishop, and W. O. Springer, *Phys. Rev. Lett.,* 1989, **44**, 1461.

11 J. D. Brock, R. J. Birgeneau, J. D. Litster, and A. Aharony, *Contemp. Phys.* 1989, **30**, 321.
12 L. E. Hough, H. T. Jung, D. Krüerke, M. S. Heberling, M. Nakata, C. D. Jones, D. Chen, D. R. Link, J. Zasadzinski, G. Heppke, J. P. Rabe, W. Stocker, E. Körblova, D. M. Walba, M. A. Glaser, and N. A. Clark, *Science,* 2009, **325**, 456.
13 D. A. Coleman, J. Fernsler, N. Chattham, M. Nakata, Y. Takanishi, E. Körblova, D. R. Link, R.-F. Shao, W. G. Jang, J. E. Maclennan, O. Mondainn-Monval, C. Boyer, W. Weissflog, G. Pelzl, L.-C. Chien, J. Zasadzinski, J. Watanabe, D. M. Walba, H. Takezoe, and N. A. Clark, *Science,* 2003, **301**, 1204.
14 W. Park, T. Ha, T.-T. Kim, A. Zep, H. Ahn, T. J. Shin, K. I. Sim, T. S. Jung, J. H. Kim, D. Pociecha, E. Gorecka, and D. K. Yoon, *NPG Asia Mater*, 2019, **11**, 45.
15 H. Kim, S. H. Ryu, M. Tuchband, T. J. Shin, E. Korblova, D. M. Walba, N. A. Clark, D. K. Yoon, *Science Advances*, 2017, **3**, e1602102.
16 S. Diele, S. Tosch, S. Mahnke, and D. Demus, *Cryt. Res. Technol.*, 1991, **26**, 809.
17 D. S. Kim and D. K. Yoon, *J. Inf. Disp.* 2018, **19**, 7-23
18 P. J. Collings and M. Hird, *Introduction to Liquid Crystals Chemistry and Physics,* Taylor & Francis, Ltd., London, 1997.
19 J. Prost and P. Barois, *J. de Chimie Physique,* 1983, **80**, 65.
20 N. A. Clark and T. P. Rieker, *Phys. Rev. A*, 1988, **37**, 1053.
21 N. A. Clark, T. P. Rieker, and J. E. Maclennan, *Ferroelectrics, 1988,* **85**, 79.
22 J. D. Brock, D. Y. Noh, B. R. Mcclain, J. D. Litster, R. J. Birgeneau, A. Aharony, P. M. Horn, and J. C. Liang, Z. *Phys. B - Condensed Matter, 1989,* **74**, 197.
23 P. S. Pershan, *Structure of Liquid Crystal Phases*, World Scientific, Singapore, 1988.
24 T. Stoebe and C. C. Huang, *Phys. Rev. E,* 1994, **49** 5238.
25 H. Iino, T. Usui, and J. Hanna, *Nat. Commun.* 2015, **6**, 6828.
26 A. Kim, K. S. Jang, J. Kim, J. C. Won, M. H. Yi, H. Kim, D. K. Yoon, T. J. Shin, M. H. Lee, J. W. Ka, and Y. H. Kim, *Adv. Mater.* 2013, **25**, 6219.
27 M. J. Han, D. Wei, Y. H. Kim, D. M. Walba, and D. K. Yoon, *ACS Central Science,* 2018, **4**, 1495.
28 I. Chuang, N. Turok, and B. Yurke, *Phys. Rev. Lett.,* 1991, **66**, 2472.
29 A. Gutierrez-Campos, G. Diaz-Leines, and R. Castillo, *J. Phys. Chem. B,* 2010, **114**, 5034.
30 S. Gurevich, E. Soule, A. Rey, L. Reven, and N. Provata, *Physical Review E*, 2014, 90, 020501.
31 J. P. Marcerou, M.P. Petrov, H. Naradikian, and H. T.Nguyen, *Liquid Crystals*, 2004, **31**, 311.
32 D. K. Yoon, J. Yoon, Y. H. Kim, M. C. Choi, J. Kim, O. Sakata, S. Kimura, M. W. Kim, I. I. Smalyukh, N. A. Clark, M. Ree, and H. T. Jung, *Phys. Rev. E* 2010, **82**, 041705.
33 D. K. Yoon, Y. H. Kim, D. S. Kim, S. D. Oh, I. I. Smalyukh, N. A. Clark, and H.-T. Jung, *Proc. Natl. Acad. Sci. U.S.A,* 2013, **110**, 19263.
34 D. S. Kim, Y. J. Cha, M. H. Kim, O. D. Lavrentovich, D. K. Yoon, *Nat. Commun.*, 2016, ***7***, 10236.
35 D. S. Kim, A. Suh, S. Yang, D. K. Yoon, *J. Colloid Interface Sci.*, 2018, **513**, 585
36 D. S. Kim, W. Lee, T. Lopez-Leon, D. K. Yoon, *Small*, 2019, **15**, 1903818.
37 A. F. Leung, *Phys. Teach.* 1980, **18**, 612.
38 S. R. Lee, D. K. Yoon, S. -H. Park, E. H. Lee, Y. H. Kim, P. Stenger, J. A. Zasadzinski, H. -T. Jung, *Langmuir*, **21**, 4989.
39 L. Ratke and P. W. Voorhees, *Growth and Coarsening*, Springer, Berlin, 2002.
40 J. S. Langer, *ReV. Mod. Phys.* 1980, **52**, 1.
41 E. Ben-Jacob, *Contemp. Phys.* 1993, **34**, 247.
42 P. C. Hohenberg and B. I. Halperin, *Rev. Mod. Phys.* 1997, **49**, 435.
43 H. Chan and I. Dierking, *Phys. Rev. E.* 2004, **70**, 021703.
44 I. M. Lifshitz, *Sov. Phys. JETP,* 1962, **15**, 939.
45 S. M. Allen and J. W. Cahn, *Acta Metall.* 1979, **27**, 1085.
46 A. J. Bray, *Adv. Phys.* 1994, **43**, 357.
47 K. Dieckmann, M. Schumacher, and H. Stegemeyer, *Liq. Cryst.* 1998, **25**, 349.